Special two-energy-two-angle approximation for bremsstrahlung

Z. M. Ding*
Department of Physics, Central Michigan University, Mt. Pleasant, Michigan 48859
and Department of Physics and Institute for Nuclear Theory, Brooklyn College of the City University of New York, Brooklyn, New York 11210

Dahang Lin and M. K. Liou
Department of Physics and Institute for Nuclear Theory, Brooklyn College of the City University of New York, Brooklyn, New York 11210
(Received 19 July 1988)

Two bremsstrahlung amplitudes in the special two-energy-two-angle approximation, which are relativistic, gauge invariant, and consistent with the soft-photon theorem, are derived for bremsstrahlung processes with or without scattering resonances. These two amplitudes include the first two terms in the series expansion of the bremsstrahlung amplitude in powers of the photon energy but they are independent of any derivative of the elastic T matrix with respect to the total energy squared s or the momentum transfer squared t. It is found that the special two-energy-two-angle approximation provides an excellent description of almost all the available $\pi^{\pm}p\gamma$ and $p^{12}C\gamma$ data.

I. INTRODUCTION

During the last decade, considerable attention has been focused on the effects of scattering resonances on bremsstrahlung emissions. Several radiative resonant scattering processes have been studied both experimentally and theoretically. Two processes whose cross sections have been systematically measured are the pion-proton bremsstrahlung ($\pi^{\pm}p\gamma$) near the $\Delta(1232)$ resonance[1] and the proton-carbon bremsstrahlung ($p^{12}C\gamma$) near both the 1.7-MeV resonance[2-4] and the 461-keV resonance.[5] Another process, the proton-oxygen bremsstrahlung ($p^{16}O\gamma$) near the 2.66-MeV resonance, has also been studied very recently by the Brooklyn group.[6] There are many good reasons for studying these radiative resonant scattering processes. In addition to the study of the off-shell effects (the most important goal in the investigation of the nucleon-nucleon bremsstrahlung[7]), these processes have been used either to study the electromagnetic properties of resonances or to measure nuclear time delay, providing information which can be used to study nuclear reactions.[8-11] In fact, values of the magnetic moment of $\Delta(1232)$, ranging from 1.6 to 9.8 $e/(2m_p)$ (m_p is the proton mass), have been extracted from the $\pi^{+}p\gamma$ [University of California at Los Angeles (UCLA)] data[1] by many authors[12-15] using various theoretical models and nuclear time delays of the order of 10^{-20} s have been extracted from the $p^{12}C\gamma$ data.[2,4,16] Moreover, since different approximate bremsstrahlung amplitudes may predict quite different cross sections in the vicinity of a resonance, the combined $\pi^{\pm}p\gamma$ and $p^{12}C\gamma$ data can also provide a very sensitive test of the validity of various theoretical approximations and models.

Among various theoretical models and approximations proposed during the past three decades for bremsstrahlung calculations, the most well-known approximations are the soft-photon approximations (SPA). The SPA, which can be used to calculate the bremsstrahlung cross section in terms of the corresponding elastic scattering amplitude, are based upon a fundamental theorem, known as the soft-photon theorem or the low-energy theorem. It was first derived by Low[17] and was generalized and extended later by many other authors.[18,19] The SPA can be divided into the following classes:[20] (i) the one-energy-one-angle approximation (OEOA), which includes Low's original SPA (Low),[17] the external-emission-dominance (EED) approximation of Nefkens and Sober,[21] and the modified SPA of Nutt, Liu, and Liou (NLL),[22] (ii) the one-energy-two-angle approximation (OETA), (iii) the two-energy-one-angle approximation (TEOA), which includes the Feshbach-Yennie approximation (FYA),[23] (iv) the two-energy-two-angle approximation (TETA), which includes the Fischer-Minkowski approximation[24] and Heller's approximation.[25] The OEOA, OETA, and TEOA have been thoroughly investigated, but a systematic study of the TETA has not yet been done.

We have studied various TETA approximations by applying them to calculate the $\pi^{\pm}p\gamma$ and $p^{12}C\gamma$ cross sections. When the results of our calculations are compared with the experimental data, we have found a special TETA approximation (referred to as TETAS) which can be used to describe almost all of the $\pi^{\pm}p\gamma$ and $p^{12}C\gamma$ data.[26] In this paper, we describe the derivation of this approximation and explain why it is a good approximation for bremsstrahlung processes in the energy region of a resonance. We also present the results of $\pi^{\pm}p\gamma$ and $p^{12}C\gamma$ cross sections calculated in the TETAS approximation. These results are compared with experimental data and with the predictions calculated in other approximations.

II. SPECIAL TWO-ENERGY-TWO-ANGLE APPROXIMATION

We consider photon emission accompanying the scattering of two particles A and B

$$A(q_i^\mu)+B(p_i^\mu)\rightarrow A(q_f^\mu)+B(p_f^\mu)+\gamma(K^\mu) .$$

Here, q_i^μ (q_f^μ) and p_i^μ (p_f^μ) are the initial (final) four-momenta for particles A and B, respectively, and K^μ is the four-momentum for the emitted photon. These five momenta satisfy energy-momentum conservation

$$q_i^\mu+p_i^\mu=q_f^\mu+p_f^\mu+K^\mu .$$

We shall first discuss the spinless case (or the case with spin but the contribution from the spin and the magnetic moment of the participating particles is negligible) and assume that particles A and B have charges Z_Ae and Z_Be, respectively. Since we are interested in the soft-photon approximation, we shall derive an approximate bremsstrahlung amplitude which can be calculated exactly in terms of the corresponding elastic T matrix and the charges Z_Ae and Z_Be. A diagram which represents the elastic scattering process is shown in Fig. 1(a).

The total bremsstrahlung amplitude M_μ consists of the external scattering amplitude M_μ^E and the internal scattering amplitude M_μ^I:

$$M_\mu=M_\mu^E+M_\mu^I . \tag{1}$$

In Fig. 2, we show five photon emission diagrams for all bremsstrahlung processes. The first four diagrams [Figs. 2(a)–(d)] represent photon emission from the four external legs (lines) and these external diagrams determine the amplitude M_μ^E. The last diagram [Fig. 2(e)] represents photon emission from all internal lines and/or vertices and it defines the amplitude M_μ^I. A general method which enables us to generate all possible soft-photon approximations is discussed in Ref. 20. The reader is referred to this reference for the details. Here, we shall focus on the TETA approximations. All TETA amplitudes depend upon two different energies and two different angles. A class of such TETA amplitudes can be written as[20]

$$M_\mu^{AB}(s_{\alpha_1\beta_1},t_{\alpha_1'\beta_1'};s_{\alpha_2\beta_2},t_{\alpha_2'\beta_2'})=A_\mu(s_{\alpha_1\beta_1},t_{\alpha_1'\beta_1'};s_{\alpha_2\beta_2},t_{\alpha_2'\beta_2'})/K+B_\mu(s_{\alpha_1\beta_1},t_{\alpha_1'\beta_1'};s_{\alpha_2\beta_2},t_{\alpha_2'\beta_2'}) , \tag{2a}$$

where

$$\begin{aligned}A_\mu/K=&Z_A\left[\frac{q_{f\mu}}{q_f\cdot K}-\frac{(q_f+p_f)_\mu}{(q_f+p_f)\cdot K}\right]T(s_{\alpha_1\beta_1},t_{\alpha_1'\beta_1'})-Z_A\left[\frac{q_{i\mu}}{q_i\cdot K}-\frac{(q_i+p_i)_\mu}{(q_i+p_i)\cdot K}\right]T(s_{\alpha_2\beta_2},t_{\alpha_1'\beta_1'})\\&+Z_B\left[\frac{p_{f\mu}}{p_f\cdot K}-\frac{(q_f+p_f)_\mu}{(q_f+p_f)\cdot K}\right]T(s_{\alpha_1\beta_1},t_{\alpha_2'\beta_2'})-Z_B\left[\frac{p_{i\mu}}{p_i\cdot K}-\frac{(q_i+p_i)_\mu}{(q_i+p_i)\cdot K}\right]T(s_{\alpha_2\beta_2},t_{\alpha_2'\beta_2'})\end{aligned} \tag{2b}$$

and

$$\begin{aligned}B_\mu=&2Z_A\frac{\beta_1}{\alpha_1+\beta_1}\left[\frac{q_{f\mu}}{q_f\cdot K}-\frac{(q_i+p_i)_\mu}{(q_i+p_i)\cdot K}\right](q_i+p_i)\cdot K\,\partial T(s_{\alpha_1\beta_1},t_{\alpha_1'\beta_1'})/\partial s_{\alpha_1\beta_1}\\&+2Z_A\frac{\alpha_2}{\alpha_2+\beta_2}\left[\frac{q_{i\mu}}{q_i\cdot K}-\frac{(q_i+p_i)_\mu}{(q_i+p_i)\cdot K}\right](q_i+p_i)\cdot K\,\partial T(s_{\alpha_2\beta_2},t_{\alpha_1'\beta_1'})/\partial s_{\alpha_2\beta_2}\\&+2Z_B\frac{\beta_1}{\alpha_1+\beta_1}\left[\frac{p_{f\mu}}{p_f\cdot K}-\frac{(q_i+p_i)_\mu}{(q_i+p_i)\cdot K}\right](q_i+p_i)\cdot K\,\partial T(s_{\alpha_1\beta_1},t_{\alpha_2'\beta_2'})/\partial s_{\alpha_1\beta_1}\\&+2Z_B\frac{\alpha_2}{\alpha_2+\beta_2}\left[\frac{p_{i\mu}}{p_i\cdot K}-\frac{(q_i+p_i)_\mu}{(q_i+p_i)\cdot K}\right](q_i+p_i)\cdot K\,\partial T(s_{\alpha_2\beta_2},t_{\alpha_2'\beta_2'})/\partial s_{\alpha_2\beta_2}\\&-2Z_A\frac{\beta_1'}{\alpha_1'+\beta_1'}\left[\frac{q_{f\mu}}{q_f\cdot K}-\frac{(q_i-q_f)_\mu}{(q_i-q_f)\cdot K}\right](q_i-p_f)\cdot K\,\partial T(s_{\alpha_1\beta_1},t_{\alpha_1'\beta_1'})/\partial t_{\alpha_1'\beta_1'}\\&+2Z_A\frac{\beta_1'}{\alpha_1'+\beta_1'}\left[\frac{q_{i\mu}}{q_i\cdot K}-\frac{(q_i-q_f)_\mu}{(q_i-q_f)\cdot K}\right](q_i-q_f)\cdot K\,\partial T(s_{\alpha_2\beta_2},t_{\alpha_1'\beta_1'})/\partial t_{\alpha_1'\beta_1'}\\&+2Z_B\frac{\alpha_2'}{\alpha_2'+\beta_2'}\left[\frac{p_{f\mu}}{p_f\cdot K}-\frac{(q_i-q_f)_\mu}{(q_i-q_f)\cdot K}\right](q_i-q_f)\cdot K\,\partial T(s_{\alpha_1\beta_1},t_{\alpha_2'\beta_2'})/\partial t_{\alpha_2'\beta_2'}\\&-2Z_B\frac{\alpha_2'}{\alpha_2'+\beta_2'}\left[\frac{p_{i\mu}}{p_i\cdot K}-\frac{(q_i-q_f)_\mu}{(q_i-q_f)\cdot K}\right](q_i-q_f)\cdot K\,\partial T(s_{\alpha_2\beta_2},t_{\alpha_2'\beta_2'})/\partial t_{\alpha_2'\beta_2'} .\end{aligned} \tag{2c}$$

In Eqs. (2b) and (2c), T is the elastic scattering T matrix,

$$s_{\alpha_n\beta_n}=(\alpha_n s_i+\beta_n s_f)/(\alpha_n+\beta_n) ,$$

$$t_{\alpha'_n\beta'_n}=(\alpha'_n t_p+\beta'_n t_q)/(\alpha'_n+\beta'_n), \quad n=1,2 ,$$

$$s_i=(q_i+p_i)^2 ,$$

$$s_f=(q_f+p_f)^2 ,$$

$$t_p=(p_f-p_i)^2 ,$$

$$t_q=(q_f-q_i)^2 ,$$

and α_n, β_n, α'_n, and β'_n $(n=1,2)$ are arbitrary real numbers. It is easy to see that the amplitudes M_μ^{AB} depend not only upon T, evaluated at four different sets of (s,t), but also upon the derivatives of T with respect to $s_{\alpha_n\beta_n}$ and $t_{\alpha'_n\beta'_n}$ $(n=1,2)$. A special TETA amplitude which is free of any derivative of T with respect to s or t can be found if we choose $\beta_1=\beta'_1=\alpha_2=\alpha'_2=0$. Thus the TETAS amplitude for spinless particles has the form

$$M_\mu^{\text{TETAS}}(s_i,s_f;t_p,t_q)=Z_A\left[\frac{q_{f\mu}}{q_f\cdot K}-\frac{(q_f+p_f)_\mu}{(q_f+p_f)\cdot K}\right]T(s_i,t_p)-Z_A T(s_f,t_p)\left[\frac{q_{i\mu}}{q_i\cdot K}-\frac{(q_i+p_i)_\mu}{(q_i+p_i)\cdot K}\right]$$
$$+Z_B\left[\frac{p_{f\mu}}{p_f\cdot K}-\frac{(q_f+p_f)_\mu}{(q_f+p_f)\cdot K}\right]T(s_i,t_q)-Z_B T(s_f,t_q)\left[\frac{p_{i\mu}}{p_i\cdot K}-\frac{(q_i+p_i)_\mu}{(q_i+p_i)\cdot K}\right] . \tag{3}$$

To understand the physical meaning of the TETAS amplitude, let us consider the $p\,^{12}\mathrm{C}\gamma$ process near a scattering resonance (around 1.7 or 0.5 MeV) as an example:

$$\mathrm{P}(p_i^\mu)+{}^{12}\mathrm{C}(q_i^\mu)\rightarrow{}^{13}\mathrm{N}^*\rightarrow\mathrm{P}(p_f^\mu)+{}^{12}\mathrm{C}(q_f^\mu)+\gamma(K^\mu) .$$

Here, we have chosen particle B to be proton and particle A to be ^{12}C, $Z_B=1$, and $Z_A=6$. Since the contribution from those terms involving spin or magnetic moment is negligible for low-energy scattering, the TETAS amplitude for the $p\,^{12}\mathrm{C}\gamma$ process can be written as

$$\mathcal{M}_\mu=\bar{u}(p_f,\nu_f)M_\mu^{\text{TETAS}}(s_i,s_f;t_p,t_q)u(p_i,\nu_i) . \tag{4}$$

Here, M_μ^{TETAS} is given by Eq. (3) and $u(p_i,\nu_i)$ [or $u(p_f,\nu_f)$] is the Dirac spinor for proton with momentum p_i (or p_f) and spin component ν_i (or ν_f). In the resonance region, an intermediate particle, ^{13}N*, is formed by the scattering of proton and carbon, and in that case the Feynman diagram given by Fig. 1(b) becomes the dominant elastic diagram. Using Fig. 1(b) as the source diagram to generate photon emission diagrams, we obtain five bremsstrahlung diagrams (as shown in Fig. 3) which dominate bremsstrahlung production in the resonance region. The elastic scattering T matrix corresponding to Fig. 1(b) has the form

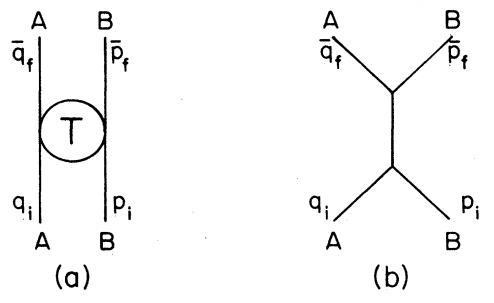

FIG. 1. (a) The graphical representation of elastic scattering. (b) The one-particle s-channel exchange diagram (the dominant elastic diagram in the resonance region).

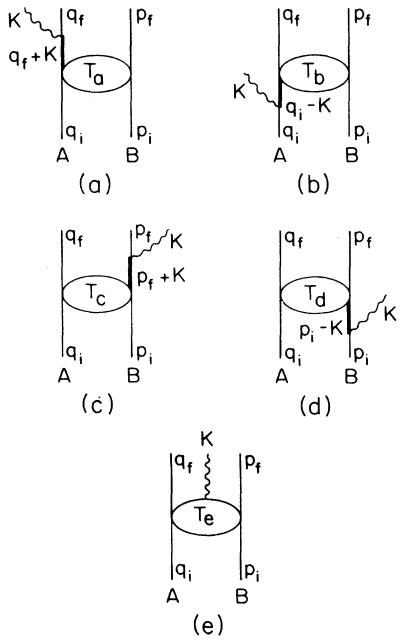

FIG. 2. Feynman diagrams for bremsstrahlung: (a)–(d) the external scattering diagrams; (e) the internal scattering diagram.

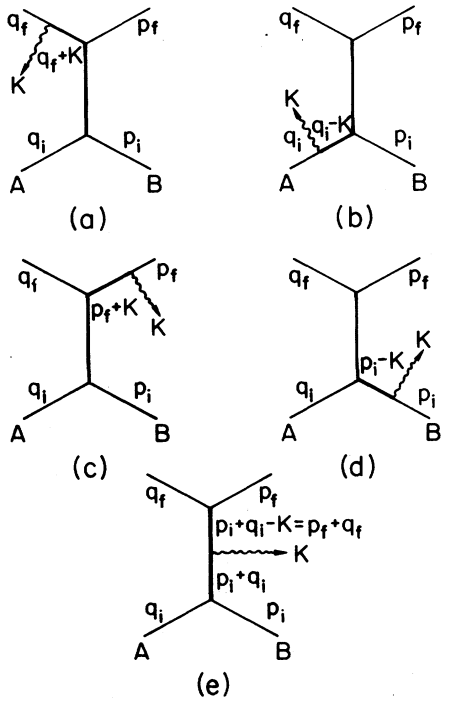

FIG. 3. Feynman diagrams for photon emission generated by the source diagram, Fig. 1(b): (a)–(d) the external emission diagrams; (e) the internal emission diagram.

$$\bar{T}(s)\equiv\Gamma[i/(s-M^{*2}+i\varepsilon)]\Gamma \ . \tag{5}$$

Here, M^* is the mass of ^{13}N*, Γ is the p-^{13}N*-^{12}C vertex, and s is the total energy squared (which can be either s_i or s_f). The external amplitude, $\bar{u}(p_f,\nu_f)\bar{M}^E_\mu u(p_i,\nu_i)$, for the Feynman diagrams in Figs. 3(a)–3(d) can be written in terms of $\bar{T}(s_i)$ and $\bar{T}(s_f)$ as

$$\bar{M}^E_\mu = Z_A\frac{q_{f\mu}}{q_f\cdot K}\bar{T}(s_i)-Z_A\bar{T}(s_f)\frac{q_{i\mu}}{q_i\cdot K} +Z_B\frac{p_{f\mu}}{p_f\cdot K}\bar{T}(s_i)-Z_B\bar{T}(s_f)\frac{p_{i\mu}}{p_i\cdot K} \ . \tag{6}$$

The internal amplitude, $\bar{u}(p_f,\nu_f)\bar{M}^I_\mu u(p_i,\nu_i)$, corresponding to Fig. 3(e) has the form

$$\bar{M}^I_\mu=\Gamma[i/(p'^2-M^{*2}+i\varepsilon)][-i(Z_A+Z_B)(p+p')_\mu] \times[i/(p^2-M^{*2}+i\varepsilon)]\Gamma \ , \tag{7}$$

where $p_\mu=(p_i+q_i)_\mu$ and $p'_\mu=p_\mu-K_\mu=p_{f\mu}+q_{f\mu}$. Applying the Brodsky-Brown decomposition identity[27] to split the amplitude $\bar{M}^I_\mu$, we obtain four quasiexternal amplitudes:

$$\bar{M}^I_\mu=Z_A\bar{T}(s_f)\frac{(q_i+p_i)_\mu}{(q_i+p_i)\cdot K}-Z_A\frac{(q_f+p_f)_\mu}{(q_f+p_f)\cdot K}\bar{T}(s_i) +Z_B\bar{T}(s_f)\frac{(q_i+p_i)_\mu}{(q_i+p_i)\cdot K}-Z_B\frac{(q_f+p_f)_\mu}{(q_f+p_f)\cdot K}\bar{T}(s_i) \ . \tag{8}$$

Combining Eqs. (6) and (8) gives

$$\bar{M}_\mu=\bar{M}^E_\mu+\bar{M}^I_\mu=Z_A\left[\frac{q_{f\mu}}{q_f\cdot K}-\frac{(q_f+p_f)_\mu}{(q_f+p_f)\cdot K}\right]\bar{T}(s_i) -Z_A\bar{T}(s_f)\left[\frac{q_{i\mu}}{q_i\cdot K}-\frac{(q_i+p_i)_\mu}{(q_i+p_i)\cdot K}\right] +Z_B\left[\frac{p_{f\mu}}{p_f\cdot K}-\frac{(q_f+p_f)_\mu}{(q_f+p_f)\cdot K}\right]\bar{T}(s_i) -Z_B\bar{T}(s_f)\left[\frac{p_{i\mu}}{p_i\cdot K}-\frac{(q_i+p_i)_\mu}{(q_i+p_i)\cdot K}\right] \ . \tag{9}$$

If we compare Eq. (9) with Eq. (3), we can see that the amplitude $M^{\rm TETAS}_\mu$ reduces to the amplitude $\bar{M}_\mu$ in the resonance region. This shows very clearly that the amplitude $M^{\rm TETAS}_\mu$ takes into account the photon emission from the charge of the intermediate particle ^{13}N*. The second term in each of the square brackets in Eq. (3) [i.e., the term which involves $(q_i+p_i)_\mu/(q_i+p_i)\cdot K$ or $(q_f+p_f)_\mu/(q_f+p_f)\cdot K$] is called the gauge term since it is required in order to make the total amplitude gauge invariant. These gauge terms represent photon emission from the charge of the intermediate particle ^{13}N*.

The TETAS amplitude given by Eq. (3) is consistent with the soft-photon theorem. Although the individual gauge terms appear to be both $0(K^{-1})$ and nonanalytic at $K=0$, the complete internal amplitude, which is the sum of all gauge terms, can be shown to be $0(K^0)$ and analytic at $K=0$. To see this, we rearrange Eq. (3) in the form

$$M^{\rm TETAS}_\mu=M^E_\mu({\rm TETAS})+M^I_\mu({\rm TETAS}) \ , \tag{10a}$$

where

$$M^E_\mu({\rm TETAS})=Z_A\frac{q_{f\mu}}{q_f\cdot K}T(s_i,t_p)-Z_AT(s_f,t_p)\frac{q_{i\mu}}{q_i\cdot K} +Z_B\frac{p_{f\mu}}{p_f\cdot K}T(s_i,t_q)-Z_BT(s_f,t_q)\frac{p_{i\mu}}{p_i\cdot K} \tag{10b}$$

and

$$M^I_\mu({\rm TETAS})=-Z_A\frac{(q_i+p_i)_\mu}{(q_i+p_i)\cdot K}[T(s_i,t_p)-T(s_f,t_p)] -Z_B\frac{(q_i+p_i)_\mu}{(q_i+p_i)\cdot K}[T(s_i,t_q)-T(s_f,t_q)] \ . \tag{10c}$$

Here, we have used the fact that $K^2=\varepsilon\cdot K=0$ and

$$(q_i+p_i)\cdot\varepsilon/(q_i+p_i)\cdot K=(q_f+p_f)\cdot\varepsilon/(q_f+p_f)\cdot K$$

(ε^μ is the photon polarization). M^E_μ(TETAS) is the external emission amplitude and M^I_μ(TETAS) is the internal amplitude, which represents photon emission from the charge of the intermediate particle as we have already discussed. If we expand $T(s_f,t_p)$ and $T(s_f,t_q)$ about s_i ($K=0$) and use the relation $s_i-s_f=2(q_i+p_i)\cdot K$, we find

$$M_\mu^I(\text{TETAS}) = -2(q_i+p_i)_\mu [Z_A \partial T(s_i,t_p)/\partial s_i + Z_B \partial T(s_i,t_q)/\partial s_i] + \cdots \tag{11}$$

which shows that the internal amplitude M_μ^I(TETAS) is of order K^0 and is independent of K^μ when $K \to 0$. Thus, M_μ^I(TETAS) has no kinematic singularity at $K=0$.

Historically, the amplitude M_μ^{TETAS} given by Eq. (3) (or an amplitude similar to M_μ^{TETAS}) has been obtained and written in various forms by many other authors. Fischer and Minkowski,[24] for example, have obtained a TETA amplitude [Eq. (40) of Ref. 24] similar but not identical to M_μ^{TETAS} for $\pi^\pm p\gamma$ processes. It is true that a large discrepancy has been found between the $\pi^\pm p\gamma$ cross sections calculated in the Fischer-Minkowski approximation and the UCLA data.[1] However, if we ignore those terms involving spin and the anomalous magnetic moment of proton in Fischer-Minkowski (FM) amplitude, we would obtain our version of the Fischer-Minkowski amplitude for spinless particles:

$$M_\mu^{\text{FM}} = M_\mu^E(\text{TETAS}) - 2(q_i+p_i)_\mu [Z_A D_{s_f} T(s_i,t_p) + Z_B D_{s_f} T(s_i,t_q)] , \tag{12}$$

where

$$D_{s_f} T(s_i,t_p) \equiv [T(s_f,t_p) - T(s_i,t_p)]/(s_f - s_i) ,$$

$$D_{s_f} T(s_i,t_q) \equiv [T(s_f,t_q) - T(s_i,t_q)]/(s_f - s_i) ,$$

and M_μ^E(TETAS) is given by Eq. (10b). The amplitude M_μ^{FM} given by Eq. (12) is identical to M_μ^{TETAS} since $(s_i - s_f) = 2(p_i+q_i)\cdot K$. If M_μ^{FM} were used by Fischer and Minkowski for the $\pi^\pm p\gamma$ calculation, they would find a very good agreement between their calculations and the UCLA data. Heller,[25] on the other hand, has used the mean value theorem for derivatives,

$$T(s_f,t_p) - T(s_i,t_p) = (s_f - s_i)\partial T(s_0,t_p)/\partial s, \quad s_f \le s_0 \le s_i$$

and

$$T(s_f,t_q) - T(s_i,t_q) = (s_f - s_i)\partial T(s_0',t_q)/\partial s, \quad s_f \le s_0' \le s_i ,$$

to rewrite Eq. (12) in the form:

$$M_\mu^H = M_\mu^E(\text{TETAS}) - 2(p_i+q_i)_\mu [Z_A \partial T(s_0,t_p)/\partial s + Z_B \partial T(s_0',t_q)/\partial s] . \tag{13}$$

Although the internal amplitude in Eq. (13) depends on the derivative of the T matrix with respect to s, Heller has pointed out in Ref. 25 that it contributes nothing since it involves a factor $(q_i+p_i)_\mu$ [or more precisely $(q_i+p_i)\cdot\varepsilon$] which vanishes in the c.m. system and in the Coulomb gauge. Other versions of the TETA amplitude similar to M_μ^{TETAS} have also been constructed and used in the nonrelativistic potential model calculations.[28]

Now, let us discuss how to modify M_μ^{TETAS} when one of the participating particles has a spin $\frac{1}{2}$ and an anomalous magnetic moment λ. Surprisingly, our study shows that the TETAS amplitude for $\pi^\pm p\gamma$ processes,

$$\pi^\pm(q_i^\mu) + P(p_i^\mu) \to \pi^\pm(q_f^\mu) + P(p_f^\mu) + \gamma(K^\mu) ,$$

can also be written in the same form as Eq. (4) with M_μ^{TETAS} given by Eq. (3) [or Eq. (10)], $Z_A = Z_B = 1$ for $\pi^+ p\gamma$ and $-Z_A = Z_B = 1$ for $\pi^- p\gamma$. The agreement between theoretical predictions and the UCLA data is found to be very good. On the other hand, it is well known that $p_{i\mu}$ and $p_{f\mu}$ must be replaced by $p_{i\mu} - R_{i\mu}$ and $p_{f\mu} - R_{f\mu}$, respectively, in order to take into account the spin and the anomalous magnetic moment λ_p of the proton. $R_{i\mu}$ and $R_{f\mu}$ can be written as

$$R_{i\mu} = \tfrac{1}{4}[\not K, \gamma_\mu] + \lambda_p \{[\not K, \gamma_\mu], \not p_i\}/(8m_p) \tag{14a}$$

and

$$R_{f\mu} = \tfrac{1}{4}[\not K, \gamma_\mu] + \lambda_p \{[\not K, \gamma_\mu], \not p_f\}/(8m_p) . \tag{14b}$$

In Eqs. (14a) and (14b), m_p is the proton mass, and we have used $[X,Y] \equiv XY - YX$ and $\{X,Y\} \equiv XY + YX$. These expressions for $R_{i\mu}$ and $R_{f\mu}$ are obtained from the following relations:

$$\bar u(p_f,v_f)\Gamma_\mu [1/(\not p_f + \not K - m_p)] = \bar u(p_f,v_f)(p_{f\mu} - R_{f\mu})/p_f\cdot K \tag{15a}$$

and

$$[1/(\not p_i - \not K - m_p)]\Gamma_\mu u(p_i,v_i) = -(1/p_i\cdot K)(p_{i\mu} - R_{i\mu}) u(p_i,v_i) , \tag{15b}$$

where

$$\Gamma_\mu = \gamma_\mu - i\lambda_p \sigma_{\mu\nu} K^\nu/(2m_p), \quad \sigma_{\mu\nu} = i[\gamma_\mu,\gamma_\nu]/2 .$$

It is easy to show that $R_i\cdot K = R_f\cdot K = 0$. If we apply the substitutions, $p_{i\mu} \to p_{i\mu} - R_{i\mu}$ and $p_{f\mu} \to p_{f\mu} - R_{f\mu}$, to both the external amplitude [M_μ^E(TETAS) given by Eq. (10b)] and the internal amplitude [M_μ^I(TETAS) given by Eq. (10c)], we obtained the following modified TETAS amplitude:

$$M_\mu(\text{TETAS}) = Z_A \left[\frac{q_{f\mu}}{q_f\cdot K} - \frac{(q_f+p_f-R_f)_\mu}{(q_f+p_f)\cdot K}\right] T(s_i,t_p) - Z_A T(s_f,t_p) \left[\frac{q_{i\mu}}{q_i\cdot K} - \frac{(q_i+p_i-R_i)_\mu}{(q_i+p_i)\cdot K}\right] + Z_B \left[\frac{p_{f\mu}-R_{f\mu}}{p_f\cdot K} - \frac{(q_f+p_f-R_f)_\mu}{(q_f+p_f)\cdot K}\right] T(s_i,t_q) - Z_B T(s_f,t_q) \left[\frac{p_{i\mu}-R_{i\mu}}{p_i\cdot K} - \frac{(q_i+p_i-R_i)_\mu}{(q_i+p_i)\cdot K}\right] . \tag{16}$$

Since $R_i \cdot K = R_f \cdot K = 0$, the modified amplitude M_μ(TETAS) is gauge invariant,

$$M_\mu(\text{TETAS})K^\mu = 0 .$$

Our study shows that the amplitude M_μ(TETAS) can be used to describe almost all the available $\pi^\pm p\gamma$ and $p\,^{12}\text{C}\gamma$ data. The contribution from those terms involving $R_{i\mu}$ and $R_{f\mu}$ is completely negligible for the $p\,^{12}\text{C}\gamma$ process but it is important for the $\pi^\pm p\gamma$ processes.

The amplitude M_μ(TETAS) given by Eq. (16) is not the only amplitude studied by us. There are other TETAS amplitudes which are also gauge invariant but none of them is better than the amplitude M_μ(TETAS). The Fischer-Minkowski amplitude is an example. Another example is an amplitude which can be obtained if we apply the substitutions, $p_{i\mu} \to p_{i\mu} - R_{i\mu}$ and $p_{f\mu} \to p_{f\mu} - R_{f\mu}$, to the external amplitude but not to the internal amplitude. It has the form

$$\begin{aligned} M'_\mu = {} & Z_A \left[\frac{q_{f\mu}}{q_f \cdot K} - \frac{(q_f + p_f)_\mu}{(q_f + p_f)\cdot K} \right] T(s_i, t_p) - Z_A T(s_f, t_p) \left[\frac{q_{i\mu}}{q_i \cdot K} - \frac{(q_i + p_i)_\mu}{(q_i + p_i)\cdot K} \right] \\ & + Z_B \left[\frac{p_{f\mu} - R_{f\mu}}{p_f \cdot K} - \frac{(q_f + p_f)_\mu}{(q_f + p_f)\cdot K} \right] T(s_i, t_q) - Z_B T(s_f, t_q) \left[\frac{p_{i\mu} - R_{i\mu}}{p_i \cdot K} - \frac{(q_i + p_i)_\mu}{(q_i + p_i)\cdot K} \right] \end{aligned} \tag{17}$$

which is slightly different from the Fischer-Minkowski amplitude [Eq. (40) of Ref. 24]. [The FM amplitude has extra terms involving $\gamma_\mu \bar{B}(s_2, t)$ and $\gamma_\mu \bar{B}(s, t)$.] The third example is an amplitude which can be obtained if we rewrite the internal amplitude M^I_μ(TETAS) in the form

$$\begin{aligned} M^I_\mu(\text{TETAS}) = \tfrac{1}{2} \Bigg\{ & -Z_A \left[\frac{(q_f + p_f)_\mu}{(q_f + p_f)\cdot K} T(s_i, t_p) + T(s_i, t_p) \frac{(q_f + p_f)_\mu}{(q_f + p_f)\cdot K} \right] \\ & + Z_A \left[T(s_f, t_p) \frac{(q_i + p_i)_\mu}{(q_i + p_i)\cdot K} + \frac{(q_i + p_i)_\mu}{(q_i + p_i)\cdot K} T(s_f, t_p) \right] \\ & - Z_B \left[\frac{(q_f + p_f)_\mu}{(q_f + p_f)\cdot K} T(s_i, t_q) + T(s_i, t_q) \frac{(q_f + p_f)_\mu}{(q_f + p_f)\cdot K} \right] \\ & + Z_B \left[T(s_f, t_q) \frac{(q_i + p_i)_\mu}{(q_i + p_i)\cdot K} + \frac{(q_i + p_i)_\mu}{(q_i + p_i)\cdot K} T(s_f, t_q) \right] \Bigg\} , \end{aligned}$$

before we apply the substitutions, $p_{i\mu} \to p_{i\mu} - R_{i\mu}$ and $p_{f\mu} \to p_{f\mu} - R_{f\mu}$. These amplitudes (and some other amplitudes) have been thoroughly studied by us and we have found that none of them is a good approximate amplitude. They predict $\pi^\pm p\gamma$ cross sections which are in poor agreement with most of the UCLA data.

The amplitude M^{TETAS}_μ given by Eq. (3) or the amplitude M_μ(TETAS) given by Eq. (16) is interesting for it depends only on the elastic T matrix, evaluated at four different sets of (s,t): (s_i, t_p), (s_f, t_p), (s_i, t_q), and (s_f, t_q), but it is independent of any derivative of T with respect to s or t. The choice of the four sets of (s,t) is fixed by the requirement of making the TETAS amplitude free of $\partial T/\partial s$ and/or $\partial T/\partial t$. Such choice is unique and natural since the four sets of (s,t) are determined by the four external emission diagrams. There are good reasons for considering the TETAS amplitude as an ideal amplitude for bremsstrahlung processes with resonances. (i) The TETAS amplitude is relativistic, gauge invariant and consistent with the soft-photon theorem. It includes the first two terms in the series expansion of the bremsstrahlung amplitude in powers of the photon energy and its internal amplitude represents the photon emission from the intermediate particle formed by the scattering of particles A and B in the resonance region. (ii) The TETAS amplitude is free of $\partial T/\partial s$ and/or $\partial T/\partial t$. If the elastic T matrix, which has been used as an input for bremsstrahlung calculations in the soft-photon approximation, varies rapidly with s and/or t in the vicinity of a resonance, then the expansion of the four half-off-shell T matrices in powers of s or t, which is the standard technique used in the derivation of a soft-photon approximation, is obviously not valid. In that case, the amplitude which is free of $\partial T/\partial s$ and/or $\partial T/\partial t$ is the only proper choice. (iii) As pointed out in Ref. 20, if a soft-photon amplitude depends upon an elastic T matrix evaluated at $s_{\alpha\beta}$ with $\alpha \neq 0$ and $\beta \neq 0$, then the amplitude must also depend upon $\partial T/\partial s_{\alpha\beta}$. In the energy region of a resonance, the bremsstrahlung spectrum calculated from this amplitude will show a giant resonant peak (or structure), which will be centered about a photon energy K_γ and will have a width Γ_γ. [The expressions for K_γ and Γ_γ are given in Appendix A of Ref. 20, Eqs. (A4) and (A9).] Since K_γ and Γ_γ are directly proportional to $(\alpha+\beta)/\beta$ if other kinematical factors (the bombarding energy, the resonant energy, and the direction of photon) are fixed, the position and the width of the peak predicted by the amplitude can be easily determined by the values of α and β. Therefore, we know how the predicted peak changes with α and β and this useful information allows us to extract the

values of α and β from the experimental data. Our study shows that any soft-photon amplitude which depends upon $s_{\alpha\beta}$ with $\alpha\neq 0$ and $\beta\neq 0$ cannot be used to describe the resonant peak observed in the $p^{12}C\gamma$ data. In other words, it is absolutely impossible to fit the $p^{12}C\gamma$ data near a resonance by adjusting the parameters α and β. The experimentally observed peak can only be described by the amplitude which depends on a T matrix evaluated at s_i (which contributes nothing to enhance the cross section around $K=K_\gamma$ since s_i is independent of K) and another T matrix evaluated at s_f [which produces a resonant peak around $K=K_\gamma$ with $(\alpha+\beta)/\beta=1$ since s_f is a function of K]. This is an unambiguous experimental evidence for choosing the two-energy approximation which depends upon s_i and s_f. The special two-energy-two-angle approximation is supported by this evidence. Furthermore, the choice of the TETAS amplitude for the $p^{12}C\gamma$ process is also theoretically justified since it reduces to the two-energy amplitude given by Eq. (9) in the energy region of a resonance. (iv) The TETAS amplitude has been tested. As we shall show in next section, the amplitude can be used to describe almost all the available $p^{12}C\gamma$ and $\pi^{\pm}p\gamma$ data. Such an excellent fit to the data cannot be obtained by using the two-energy-one-angle approximation or other approximations.

III. BREMSSTRAHLUNG CROSS SECTION

The differential cross section for $\pi^{\pm}p\gamma$ can be written as

$$\begin{aligned}\sigma_{\pi p\gamma}&\equiv d^3\sigma/d\Omega_\pi d\Omega_\gamma dK\\&=(2\pi)^{-5}\int\delta^4(q_i+p_i-q_f-p_f-K)\\&\quad\times[\tfrac{1}{2}\Sigma_{\text{pol,spin}}(\mathcal{M}_\mu\varepsilon^\mu)^\dagger(\mathcal{M}^\mu\varepsilon_\mu)]\\&\quad\times J_{\pi p\gamma}d^4F_{\pi p\gamma}\ ,\end{aligned}\tag{18}$$

where

$$J_{\pi p\gamma}=e^2m_p^2/[(p_i\cdot q_i)^2-m_\pi^2m_p^2]^{1/2}\ ,$$

$$d^4F_{\pi p\gamma}=(q_f^2dq_f/2E_\pi)(d^3\mathbf{p}_f/2E_p)(K^2/2K)\ ,$$

$$E_\pi=(m_\pi^2+\mathbf{q}_f^2)^{1/2}\ ,$$

$$E_p=(m_p^2+\mathbf{p}_f^2)^{1/2}\ ,$$

$$\mathcal{M}_\mu=\bar{u}(p_f,v_f)M_\mu(\text{TETAS})u(p_i,v_i)$$

or

$$\bar{u}(p_f,v_f)M_\mu^{\text{TETAS}}u(p_i,v_i)\ ,$$

m_π is the mass of pion, and M_μ(TETAS) and M_μ^{TETAS} are given by Eqs. (16) and (3), respectively. The expression given by Eq. (18) can also be used to define the differential cross section for $p^{12}C\gamma$,

$$\sigma_{pC\gamma}\equiv d^3\sigma/d\Omega_p d\Omega_\gamma dK\ ,\tag{19a}$$

if $J_{\pi p\gamma}$ and $d^4F_{\pi p\gamma}$ are replaced by $J_{pC\gamma}$ and $d^4F_{pC\gamma}$. Here,

$$J_{pC\gamma}=e^2m_p^2/[(p_i\cdot q_i)^2-m_p^2m_C^2]^{1/2}\ ,$$

$$d^4F_{pC\gamma}=(p_f^2dp_f/2E_p)(d^3\mathbf{q}_f/2E_C)(K^2/2K)\ ,$$

$$E_C=(m_C^2+\mathbf{q}_f^2)^{1/2}\ ,$$

and m_C is the mass of carbon. To compare with the Brooklyn data,[3,5] we have also calculated the ratio of the bremsstrahlung cross sectin ($\sigma_{pC\gamma}$) to the elastic $p^{12}C$ cross section (σ_{el}^{pC}):

$$\sigma_{\text{rel}}^{pC\gamma}=\sigma_{pC\gamma}/\sigma_{\text{el}}^{pC}\ .\tag{19b}$$

As we have already mentioned, the TETAS amplitude depends upon the elastic scattering T matrix evaluated at four sets of (s,t): (s_i,t_p), (s_i,t_q), (s_f,t_p), and (s_f,t_q). In other words, $T(s_i,t_p)$, $T(s_i,t_q)$, $T(s_f,t_p)$, and $T(s_f,t_q)$ have been used as an input in our bremsstrahlung calculations. Since how to calculate these T matrices without ambiguity is also an important part of this work, let us briefly discuss how they are calculated in the c.m. system. We use the $\pi^{\pm}p\gamma$ process as an example.

For the πp elastic process,

$$\pi^{\pm}(q_i^\mu)+\text{P}(p_i^\mu)\rightarrow\pi^{\pm}(\bar{q}_f^{\,\mu})+\text{P}(\bar{p}_f^{\,\mu})\ ,$$

the elastic T matrix has the form

$$T(s,t)=A(s,t)+\tfrac{1}{2}(\not{q}_i+\not{\bar{q}}_f)B(s,t)\ ,\tag{20}$$

where

$$s=(q_i+p_i)^2=(\bar{q}_f+\bar{p}_f)^2\ ,$$

$$t=(q_i-\bar{q}_f)^2=(p_i-\bar{p}_f)^2\ .$$

In the c.m. system, q_i^μ and $\bar{q}_f^{\,\mu}$ can be written as

$$q_i^\mu=[(m_\pi^2+q_{\text{c.m.}}^2)^{1/2},0,0,q_{\text{c.m.}}]\tag{21a}$$

and

$$\bar{q}_f^{\,\mu}=[(m_\pi^2+q_{\text{c.m.}}^2)^{1/2},-q_{\text{c.m.}}\sin\theta_{\text{c.m.}},0,q_{\text{c.m.}}\cos\theta_{\text{c.m.}}]\ ,\tag{21b}$$

where

$$q_{\text{c.m.}}=\{[s-(m_\pi+m_p)^2][s-(m_p-m_\pi)^2]/4s\}^{1/2}\tag{21c}$$

and

$$\cos\theta_{\text{c.m.}}=1+t/(2q_{\text{c.m.}}^2)\ .\tag{21d}$$

The expression for $\bar{q}_f^{\,\mu}$ is chosen in such a way that the scattered pion in the lab system has a direction $(\theta_\pi,\phi_\pi)=(50.5°,180°)$, the direction used in the UCLA experiment. From s, the total c.m. energy is given by

$$w=s^{1/2}\ .$$

Thus for a given (s,t), the c.m. momentum $q_{\text{c.m.}}$, the total c.m. energy w and the c.m. scattering angle $\theta_{\text{c.m.}}$ can be defined. What we should emphasize here is that $q_{\text{c.m.}}$, w, and $\theta_{\text{c.m.}}$ can also be obtained from the two-body kinematics based on the energy-momentum conservation in the c.m. system,

$$q_{i\text{c.m.}}^\mu+p_{i\text{c.m.}}^\mu=\bar{q}_{f\text{c.m.}}^{\,\mu}+\bar{p}_{f\text{c.m.}}^{\,\mu}\ .$$

That is, we have

$$|\mathbf{q}_{ic.m.}|=|\bar{\mathbf{q}}_{fc.m.}|=q_{c.m.} ,$$
$$q^0_{ic.m.}+p^0_{ic.m.}=\bar{q}^{\,0}_{fc.m.}+\bar{p}^{\,0}_{fc.m.}=w ,$$

and

$$\mathbf{q}_{ic.m.}\cdot\bar{\mathbf{q}}_{fc.m.}/(|\mathbf{q}_{ic.m.}||\bar{\mathbf{q}}_{fc.m.}|)=\cos\theta_{c.m.} .$$

The amplitudes $A(s,t)$ and $B(s,t)$ can be written as functions of w and $\theta_{c.m.}$, and the complete πp elastic T matrix $T(s,t)$ can evaluated by using πp phase shifts and inelasticities.

Care must be taken in treating $T(s_i,t_p)$, $T(s_i,t_q)$, $T(s_f,t_p)$, and $T(s_f,t_q)$ as elastic T matrices since they are originally derived from four half-off-shell T matrices for the bremsstrahlung process. Let us discuss an obvious ambiguity. From s_i and s_f, we can define two c.m. momenta,

$$q^i_{c.m.}=\{[s_i-(m_\pi+m_p)^2][s_i-(m_p-m_\pi)^2]/4s_i\}^{1/2} , \tag{22a}$$

$$q^f_{c.m.}=\{[s_f-(m_\pi+m_p)^2][s_f-(m_p-m_\pi)^2]/4s_f\}^{1/2} , \tag{22b}$$

and two total c.m. energies

$$w^i=s_i^{1/2} , \tag{23a}$$
$$w^f=s_f^{1/2} . \tag{23b}$$

On the other hand, from the three-body kinematics (or the energy-momentum conservation) in the c.m. system,

$$q^\mu_{ic.m.}+p^\mu_{ic.m.}=q^\mu_{fc.m.}+p^\mu_{fc.m.}+K^\mu_{c.m.} , \tag{24}$$

we can also obtain two c.m. momenta, $\mathbf{q}_{ic.m.}$ and $\mathbf{q}_{fc.m.}$, and two total c.m. energies, $q^0_{ic.m.}+p^0_{ic.m.}$ and $q^0_{fc.m.}+p^0_{fc.m.}$. It is easy to show that

$$q^f_{c.m.}\neq|\mathbf{q}_{fc.m.}|\neq|\mathbf{q}_{ic.m.}-\mathbf{K}_{c.m.}|$$

and

$$w^f\neq q^0_{fc.m.}+p^0_{fc.m.}\neq q^0_{ic.m.}+p^0_{ic.m.} . \tag{25a}$$

Thus, two sets of the total c.m. energy, the c.m. momentum and the scattering angle can be obtained: one from a given (s,t) and another one from the three-body kinematics, Eq. (24). The fact that these two sets are different is not surprising, but it would create a problem if we wish to evaluate $T(s_f,t_p)$, for example, from the following expression:

$$T(s_f,t_p)=A(s_f,t_p)+\tfrac{1}{2}(\not{q}_{ic.m.}+\not{q}_{fc.m.}-\not{K}_{c.m.})B(s_f,t_p) . \tag{25b}$$

Since $T(s_f,t_p)$ has been treated as an elastic T matrix evaluated at (s_f,t_p), it should be evaluated at the total c.m. energy and the scattering angle determined by s_f and t_p. That is, w^f given by Eq. (23b), $q^f_{c.m.}$ given by Eq. (22b), and the scattering angle

$$\bar{\theta}^p_{c.m.}=\cos^{-1}[1+t_p/(2q^{f\,2}_{c.m.})]$$

should be used to calculate $T(s_f,t_p)$. This can be done for both $A(s_f,t_p)$ and $B(s_f,t_p)$ without any difficulty but not for the factor

$$\tfrac{1}{2}(\not{q}_{ic.m.}+\not{q}_{fc.m.}-\not{K}_{c.m.})$$

in Eq. (25b). This factor can only be calculated by solving Eq. (24), i.e., the three-body kinematics must be used. This not only means that Eq. (25b) cannot be calculated consistently but also implies that $T(s_f,t_p)$ has no longer been treated as an exact elastic T matrix [since

$$|\mathbf{q}_{fc.m.}|\neq|\mathbf{q}_{ic.m.}-\not{K}_{c.m.}|$$

and

$$(q^0_{fc.m.}+p^0_{fc.m.})\neq(q^0_{ic.m.}+p^0_{ic.m.})$$

as shown in Eq. (25a)].

Next, let us show that Eq. (11), an important property of the internal amplitude, cannot be obtained if Eq. (25b) and the following expressions for T matrices:

$$T(s_i,t_p)=A(s_i,t_p)+\tfrac{1}{2}(\not{q}_{ic.m.}+\not{q}_{fc.m.}+\not{K}_{c.m.})B(s_i,t_p) , \tag{25c}$$

$$T(s_i,t_q)=A(s_i,t_q)+\tfrac{1}{2}(\not{q}_{ic.m.}+\not{q}_{fc.m.})B(s_i,t_q) , \tag{25d}$$

and

$$T(s_f,t_q)=A(s_f,t_q)+\tfrac{1}{2}(\not{q}_{ic.m.}+\not{q}_{fc.m.})B(s_f,t_q) , \tag{25e}$$

are used in Eq. (10c). To obtain Eq. (11) from Eq. (10c), $T(s_f,t_p)$ and $T(s_f,t_q)$ must be expanded about s_i. Such expansions can be done only if $T(s_f,t_p)$ is a function of s_f and t_p and $T(s_f,t_q)$ is a function of s_f and t_q. It is obvious that the factor

$$\tfrac{1}{2}(\not{q}_{ic.m.}+\not{q}_{fc.m.}-\not{K}_{c.m.})$$

in Eq. (25b) for $T(s_f,t_p)$, for example, is not a function of s_f and t_p even though $A(s_f,t_p)$ and $B(s_f,t_p)$ are functions of s_f and t_p. To see what we would obtain if T matrices defined by Eqs. (25b)–(25e) are used in Eq. (10c), let us use Eqs. (25b) and (25c) to calculate the first term in Eq. (10c). We find

$$I\equiv-Z_A\frac{(q_i+p_i)_\mu}{(q_i+p_i)\cdot K}[T(s_i,t_p)-T(s_f,t_p)]$$
$$=-Z_A\frac{(q_i+p_i)_\mu}{(q_i+p_i)\cdot K}\{[A(s_i,t_p)-A(s_f,t_p]+\tfrac{1}{2}(\not{q}_{ic.m.}+\not{q}_{fc.m.})[B(s_i,t_p)-B(s_f,t_p)]+\tfrac{1}{2}\not{K}_{c.m.}[B(s_i,t_p)+B(s_f,t_p)]\} . \tag{25f}$$

If we expand $A(s_f,t_p)$ and $B(s_f,t_p)$ about s_i and use the relation $s_i-s_f=2(p_i+q_i)\cdot K$ again, we obtain

$$I=-2Z_A(q_i+p_i)_\mu[\partial A(s_i,t_p)/\partial s_i+\tfrac{1}{2}(\not{q}_{ic.m.}+\not{q}_{fc.m.})\partial B(s_i,t_p)/\partial s_i]$$
$$-Z_A(q_i+p_i)_\mu[\not{K}_{c.m.}/(q_i+p_i)\cdot K]B(s_i,t_p)+\cdots . \tag{25g}$$

This result is quite different from the first term of Eq. (11) mainly because Eq. (25g) includes an extra term, $\not{K}_{c.m.}/(q_i+p_i)\cdot K$, which is zeroth order in K but is not independent of K. Finally, our numerical study shows that calculation based on those T matrices defined by Eqs. (25b)–(25e) gives a large resonant peak for most of the $\pi^{\pm}p\gamma$ spectra, in disagreement with the UCLA data which show no resonant peak. To avoid the ambiguity, inconsistency and the violation of the soft-photon theorem mentioned above, we have introduced a new treatment in this work.

In our calculation, we have used $q^i_{c.m.}$ [as defined in (22a)], t_p, and t_q to define two c.m. scattering angles,

$$\theta^p_{c.m.}=\cos^{-1}[1+t_p/(2q^{i2}_{c.m.})] \tag{26a}$$

and

$$\theta^q_{c.m.}=\cos^{-1}[1+t_q/(2q^{i2}_{c.m.})] . \tag{26b}$$

We then use $q^i_{c.m.}$, $q^f_{c.m.}$, w^i, w^f, $\theta^p_{c.m.}$, and $\theta^q_{c.m.}$, [defined by (22a), (22b), (23a), (23b), (26a), and (26b), respectively] to write the following expressions for the four elastic T matrices:

(i)

$$T(s_i,t_p)=A(w^i,\theta^p_{c.m.})+\tfrac{1}{2}(\not{q}_{iip}+\not{q}_{fip})B(w^i,\theta^p_{c.m.}) ,$$

where

$$q^\mu_{iip}=\{[m_\pi^2+(q^i_{c.m.})^2]^{1/2},0,0,q^i_{c.m.}\},\quad q^\mu_{fip}=\{[m_\pi^2+(q^i_{c.m.})^2]^{1/2},-q^i_{c.m.}\sin\theta^p_{c.m.},0,q^i_{c.m.}\cos\theta^p_{c.m.}\} ,$$

(ii)

$$T(s_i,t_q)=A(w^i,\theta^q_{c.m.})+\tfrac{1}{2}(\not{q}_{iiq}+\not{q}_{fiq})B(w^i,\theta^q_{c.m.}) ,$$

where

$$q^\mu_{iiq}=q^\mu_{iip}=\{[m_\pi^2+(q^i_{c.m.})^2]^{1/2},0,0,q^i_{c.m.}\},\quad q^\mu_{fiq}=\{[m_\pi^2+(q^i_{c.m.})^2]^{1/2},-q^i_{c.m.}\sin\theta^q_{c.m.},0,q^i_{c.m.}\cos\theta^q_{c.m.}\} ,$$

(iii)

$$T(s_f,t_p)=A(w^f,\theta^p_{c.m.})+\tfrac{1}{2}(\not{q}_{ifp}+\not{q}_{ffp})B(w^f,\theta^p_{c.m.}) ,$$

where

$$q^\mu_{ifp}=\{[m_\pi^2+(q^f_{c.m.})^2]^{1/2},0,0,q^f_{c.m.}\},\quad q^\mu_{ffp}=\{[m_\pi^2+(q^f_{c.m.})^2]^{1/2},-q^f_{c.m.}\sin\theta^p_{c.m.},0,q^f_{c.m.}\cos\theta^p_{c.m.}\} ,$$

and

(iv)

$$T(s_f,t_q)=A(w^f,\theta^q_{c.m.})+\tfrac{1}{2}(\not{q}_{ifq}+\not{q}_{ffq})B(w^f,\theta^q_{c.m.})$$

where

$$q^\mu_{ifq}=q^\mu_{ifp}=\{[m_\pi^2+(q^f_{c.m.})^2]^{1/2},0,0,q^f_{c.m.}\},\quad q^\mu_{ffq}=\{[m_\pi^2+(q^f_{c.m.})^2]^{1/2},-q^f_{c.m.}\sin\theta^q_{c.m.},0,q^f_{c.m.}\cos\theta^q_{c.m.}\} .$$

It should be pointed out that we have not used scattering angles,

$$\bar\theta^p_{c.m.}=\cos^{-1}[1+t_p/(2q^{f2}_{c.m.})]$$

and

$$\bar\theta^q_{c.m.}=\cos^{-1}[1+t_q/(2q^{f2}_{c.m.})] ,$$

for $T(s_f,t_p)$ and $T(s_f,t_q)$, respectively. Were we to use $\theta^p_{c.m.}$, $\theta^q_{c.m.}$, $\bar\theta^p_{c.m.}$, and $\bar\theta^q_{c.m.}$ for $T(s_i,t_p)$, $T(s_i,t_q)$, $T(s_f,t_p)$, and $T(s_f,t_q)$, respectively, then we would have

the special two-energy-four-angle approximation rather than the TETAS. The special two-energy-four-angle approximation is also a good approximation except that the cross section cannot be calculated when the photon energy is greater than about 100 MeV for the $\pi^{\pm}p\gamma$ cases. This is because $\bar{\theta}^{p}_{\text{c.m.}}$ and $\bar{\theta}^{q}_{\text{c.m.}}$ cannot be defined for $K \geq 100$ MeV.

IV. RESULTS AND COMPARISON WITH EXPERIMENT

We have used Eq. (18) to calculate the $\pi^{\pm}p\gamma$ cross sections, $\sigma_{\pi p\gamma}$, and have used Eq. (19b) to calculate the relative $p^{12}C\gamma$ cross sections, $\sigma^{pC\gamma}_{\text{rel}}$. Two different sets of $\pi^{\pm}p\gamma$ cross sections have been calculated depending upon which TETAS amplitude, M^{TETAS}_{μ} of Eq. (3) (for two spin-0 particles) or M_{μ}(TETAS) of Eq. (16) (for a spin-$\frac{1}{2}$–spin-0 system), is used. Surprisingly, it turns out that the amplitudes M^{TETAS}_{μ} and M_{μ}(TETAS) predict very similar results (which are in excellent agreement with the UCLA data) for many photon counters even though the contribution from each term involving $R_{i\mu}$ or $R_{f\mu}$ is not negligible for the $\pi^{\pm}p\gamma$ processes near the Δ resonance. This implies that cancellation among those terms involving $R_{i\mu}$ and $R_{f\mu}$ exists. Some $\pi^{\pm}p\gamma$ spectra calculated with the amplitude M^{TETAS}_{μ} are shown in Figs. 4–6. We use the amplitude M_{μ}(TETAS) for most of our $\pi^{\pm}p\gamma$ calculations mainly because it takes into account the magnetic moment of proton and also because the overall agreement between theory and experiment is better if M_{μ}(TETAS) is used. Some $\pi^{\pm}p\gamma$ spectra (from $G1$ to $G19$) calculated with M_{μ}(TETAS) are shown in Figs. 7–14. Since the contribution from $R_{i\mu}$ and $R_{f\mu}$ terms can be completely ignored, only one set of $\sigma^{pC\gamma}_{\text{rel}}$ has been obtained using either the amplitude M^{TETAS}_{μ} or the amplitude M_{μ}(TETAS) for calculations. Some of these calculations are exhibited in Figs. 15 and 16.

As we have already mentioned in the Introduction, both the $\pi^{\pm}p\gamma$ processes and the $p^{12}C\gamma$ process have been studied experimentally and the combined $\pi^{\pm}p\gamma$ and $p^{12}C\gamma$ data have been used to test the validity of various theoretical approximations and models. The fact that the combined data cannot be completely described by either the OEOA or OETA approximation is almost well established.[20] Briefly, the OETA approximation has been applied to calculate the $\pi^{\pm}p\gamma$ spectra by the UCLA group in order to describe the spectra measured by them. They have found that the calculated spectra at 298 MeV rise steeply with increasing photon energy above $K=80$ MeV, in complete disagreement with their experimental result [see Figs. 4(d) or 7(c)]. We repeated the calculation and obtained essentially the same result. We have also applied the Low approximation to calculate the $p^{12}C\gamma$ cross sections at 1.88 MeV for a scattering angle of 155°

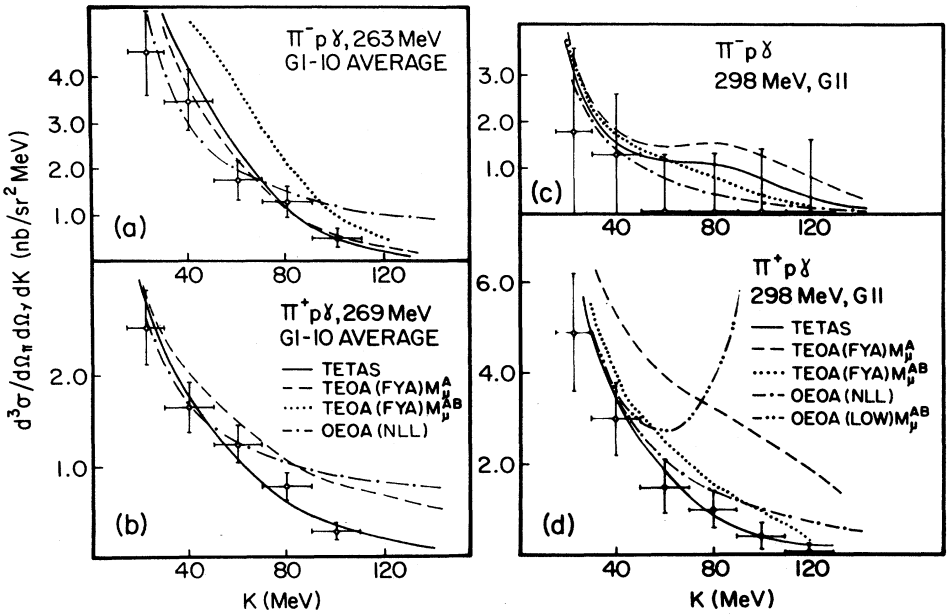

FIG. 4. Comparison of various theoretical predictions with the $\pi^{\pm}p\gamma$ data, (a) at 263 MeV (the averaged $\pi^{-}p\gamma$ cross section over the ten photon counters $G1-G10$), (b) at 269 MeV (the averaged $\pi^{+}p\gamma$ cross section over the photon counters $G1-G10$), (c) at 298 MeV ($\pi^{-}p\gamma$) for the photon counter $G11$, and (d) at 298 MeV ($\pi^{+}p\gamma$) for the photon counter $G11$. The solid curves represent the result of the TETAS calculation using the amplitude M^{TETAS}_{μ} given by Eq. (3). The dashed curves and the dotted curves represent the result of the FYA calculation using the amplitude M^{A}_{μ}(FYA) [Eq. (A1) in the Appendix] and the amplitude M^{AB}_{μ}(FYA) [Eq. (A2) in the Appendix], respectively. The dash-dotted curves are calculated in the NLL approximation and the dash-double-dotted curves are calculated in the Low approximation. The experimental $\pi^{\pm}p\gamma$ data are from Ref. 1.

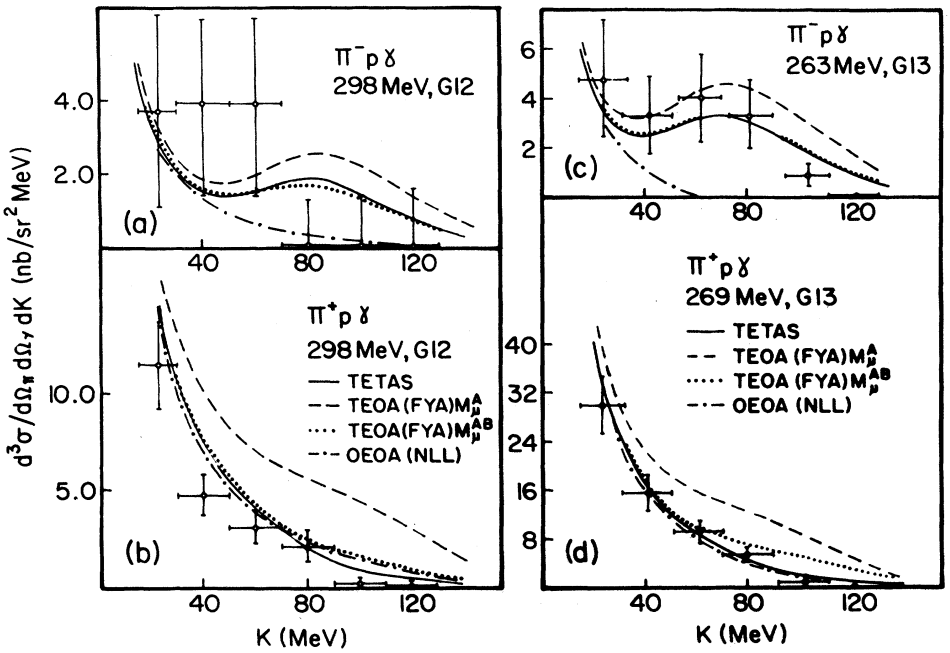

FIG. 5. Same as Fig. 4, but (a) at 298 MeV ($\pi^- p\gamma$) for $G12$, (b) at 298 MeV ($\pi^+ p\gamma$) for $G12$, (c) at 263 MeV ($\pi^- p\gamma$) for $G13$, and (d) at 269 MeV ($\pi^+ p\gamma$) for $G13$.

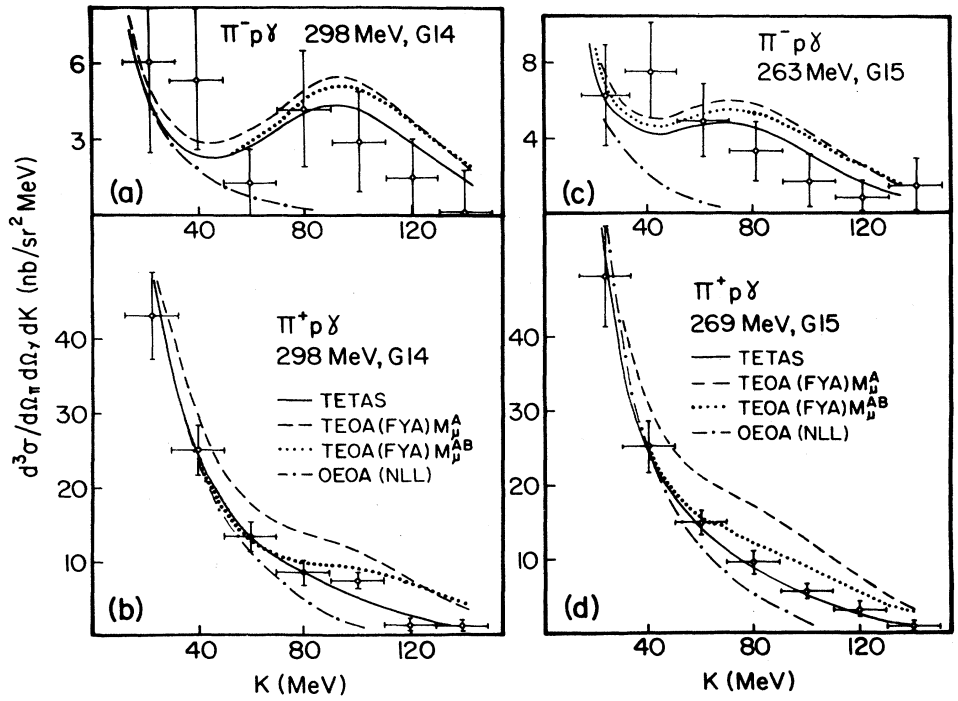

FIG. 6. Same as Fig. 4, but (a) at 298 MeV ($\pi^- p\gamma$) for $G14$, (b) at 298 MeV ($\pi^+ p\gamma$) for $G14$, (c) at 263 MeV ($\pi^- p\gamma$) for $G15$, and (d) at 269 MeV ($\pi^+ p\gamma$) for $G15$.

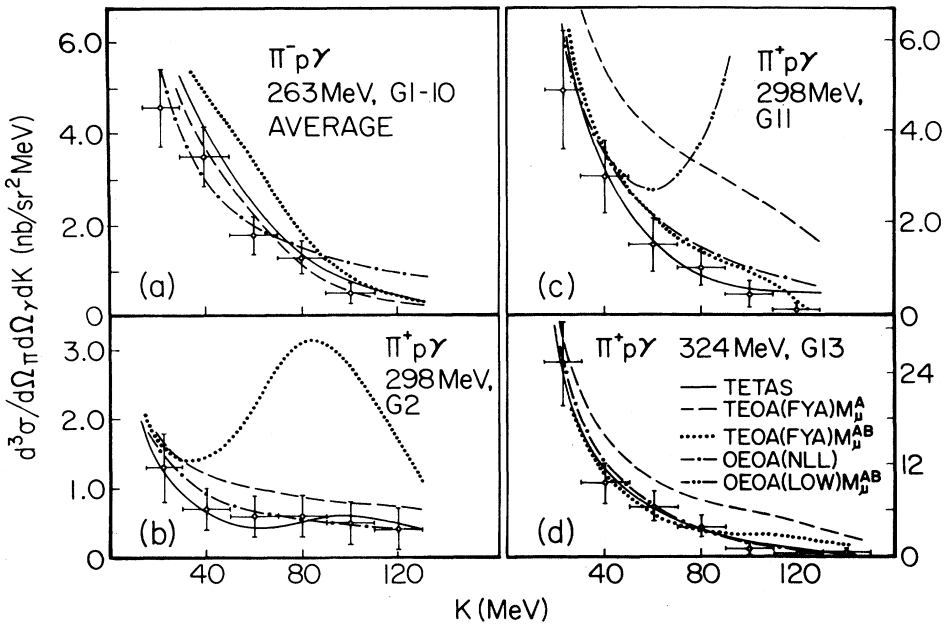

FIG. 7. Comparison of various theoretical predictions with the $\pi^{\pm}p\gamma$ data (a) at 263 MeV (the averaged $\pi^{-}p\gamma$ cross section over the ten photon counters $G1-G10$, (b) at 298 MeV for the photon counter $G2$, (c) at 298 MeV for the photon counter $G11$, and (d) at 324 MeV for the photon counter $G13$. The solid curves represent the result of the TETAS calculation using the amplitude M_{μ}(TETAS) given by Eq. (16). The dashed curves and the dotted curves represent the result of the FYA calculation using the amplitude M_{μ}^{A}(FYA) [Eq. (A1) in the Appendix with the substitutions $p_{i\mu}\rightarrow p_{i\mu}-R_{i\mu}$ and $p_{f\mu}\rightarrow p_{f\mu}-R_{f\mu}$] and the amplitude M_{μ}^{AB}(FYA) [Eq. (A2) in the Appendix with the substitutions $p_{i\mu}\rightarrow p_{i\mu}-R_{i\mu}$ and $p_{f\mu}\rightarrow p_{f\mu}-R_{f\mu}$], respectively. The dash-dotted curves are calculated in the NLL approximation and the dash-double-dotted curves are calculated in the Low approximation. The experimental $\pi^{\pm}p\gamma$ data are from Ref. 1.

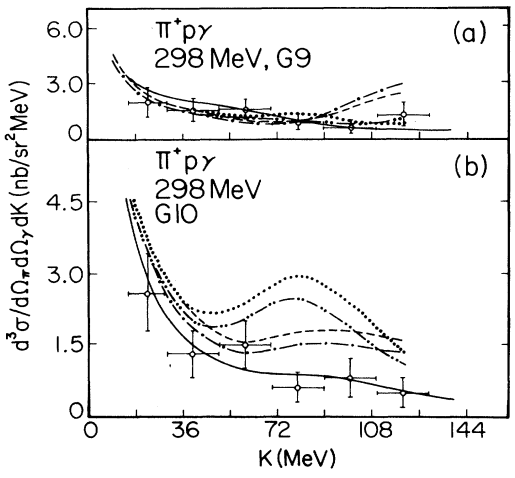

FIG. 8. A comparison of the TETAS calculation using the amplitude M_{μ}(TETAS) given by Eq. (16) with the calculation of Heller *et al.* using the MIT model. The solid curves are calculated in the TETAS approximation and the other four curves (obtained from Fig. 16 of the Ref. 14) are the MIT calculation; dotted curve: MIT model II, $\mu_{\Delta}/\mu_{p}=3$; dash-double-dotted curve: MIT model I, $\mu_{\Delta}/\mu_{p}=3$; dashed curve MIT model II, $\mu_{\Delta}/\mu_{p}=2$; and dash-dotted curve: MIT model I, $\mu_{\Delta}/\mu_{p}=2$. The experimental $\pi^{+}p\gamma$ data are from Ref. 1.

and we have found that the calculated cross sections show a giant resonance peak around $K=270$ keV, which is quite different from the small peak observed experimentally around $K=135$ keV [see Fig. 16(b)]. The EED approximation, on the other hand, can be used to describe most of the $\pi^{\pm}p\gamma$ data, but (just like the Low approximation) it fails to fit the $p^{12}C\gamma$ data near the 1.7-MeV or the 0.5-MeV resonance [see Fig. 16(b)]. Finally, the NLL approximation does not predict any resonant structure in the resonance region; it always gives a typical smooth spectra with $1/K$ dependence. Therefore, it cannot be used to describe the structure observed in the $p^{12}C\gamma$ spectra even though it works remarkably well for the $\pi^{\pm}p\gamma$ case (see Figs. 4–7). In short, the one-energy approximation (either OEOA or OETA) is inadequate to describe the combined data.

It is evident that the combined data can only be described by the two-energy approximations, which include the TEOA approximations and the TETA approximations. Since the Fischer-Minkowski amplitude, the amplitude M'_{μ} given by Eq. (17) and other amplitudes predict $\pi^{\pm}p\gamma$ cross sections which are in poor agreement with most of the UCLA data, we shall focus on the comparison between the FYA (a typical TEOA approximation) and the TETAS approximation [using the amplitude given by Eq. (3) or (16)] in this work. The expressions for the FYA amplitude are given in the Appendix. Some ex-

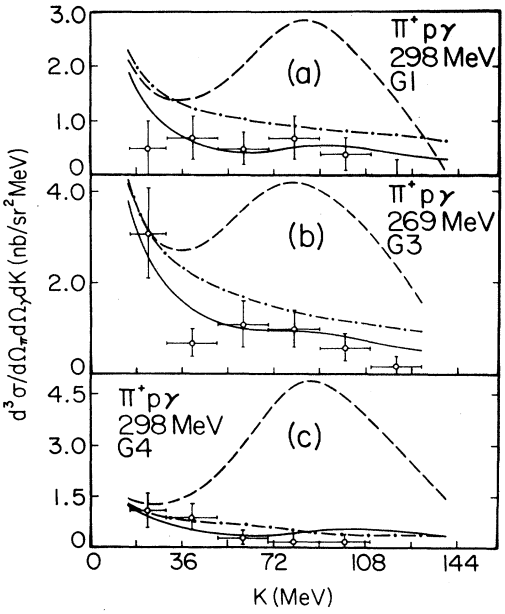

FIG. 9. The $\pi^+ p\gamma$ cross section as a function of photon energy K (a) at 298 MeV for the photon counter $G1$, (b) at 269 MeV for $G3$, and (c) at 298 MeV for $G4$. The solid curves represent the calculation using the amplitude M_μ(TETAS) given by Eq. (16). The dashed curves and the dash-dotted curves are the result of calculation using the amplitude M_μ^{AB}(FYA) [Eq. (A2) in the Appendix with the substitutions $p_{i\mu}\rightarrow p_{i\mu}-R_{i\mu}$ and $p_{f\mu}\rightarrow p_{f\mu}-R_{f\mu}$] and the amplitude M_μ^{A}(FYA) [Eq. (A1) in the Appendix with the substitutions $p_{i\mu}\rightarrow p_{i\mu}-R_{i\mu}$ and $p_{f\mu}\rightarrow p_{f\mu}-R_{f\mu}$], respectively. The experimental $\pi^+ p\gamma$ data are from Ref. 1.

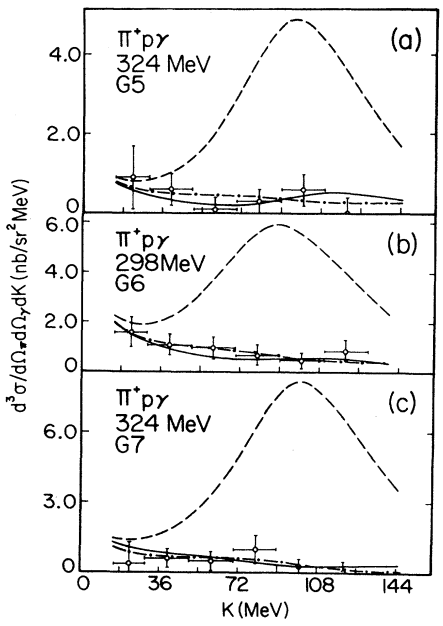

FIG. 10. Same as Fig. 9, but (a) at 324 MeV for $G5$, (b) at 298 MeV for $G6$, and (c) at 324 MeV for $G7$.

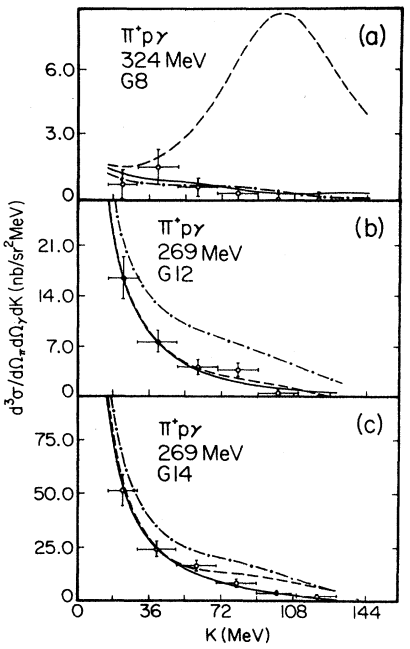

FIG. 11. Same as Fig. 9, but (a) at 324 MeV for $G8$, (b) at 269 MeV for $G12$, and (c) at 269 MeV for $G14$.

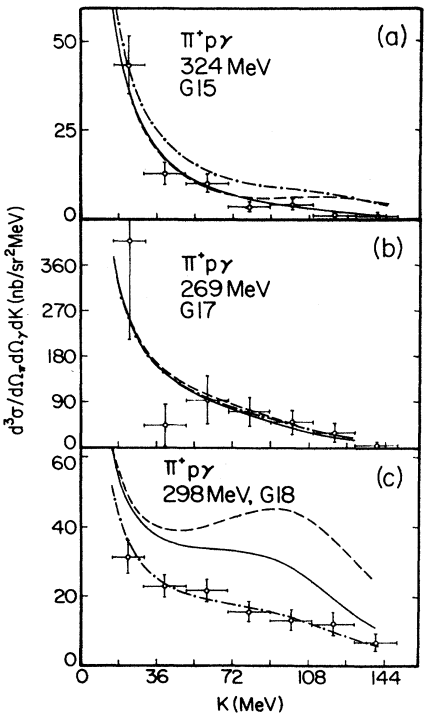

FIG. 12. Same as Fig. 9, but (a) at 324 MeV for $G15$, (b) at 269 MeV for $G17$, and (c) at 298 MeV for $G18$.

amples of such comparison can be found in Figs. 4–7 and 9–14. This comparison reveals two interesting features: (i) For the $\pi^+ p\gamma$ process, except for the photon counter $G18$ (and $G19$ for some cases), most of spectra predicted by Eq. (18) with the amplitude M_μ^{TETAS} given by Eq. (3) are in excellent agreement with the UCLA data (see Figs. 4–6) while the spectra calculated with the amplitude M_μ(TETAS) given by Eq. (16) are consistently in excellent agreement with the data (see Figs. 7–14). As for the FYA predictions, the spectra calculated with the amplitude M_μ^{AB}(FYA) [given by Eq. (A2) in the Appendix] are in excellent agreement with the data for the photon counters $G11-G17$, but the agreement becomes poor for the other counters, $G1-G10$, $G18$, and $G19$. The predictions using the amplitude M_μ^{A}(FYA) [given by Eq. (A1) in the Appendix], on the contrary, are in poor agreement with the data for the counters $G11-G17$, but the agreement is either good or excellent for the rest of the photon counters. (ii) For the $\pi^- p\gamma$ process, both the TETAS approximation [using either M_μ^{TETAS} or M_μ(TETAS)] and the FYA approximation predict about the same results, which are in very good agreement with the UCLA data,

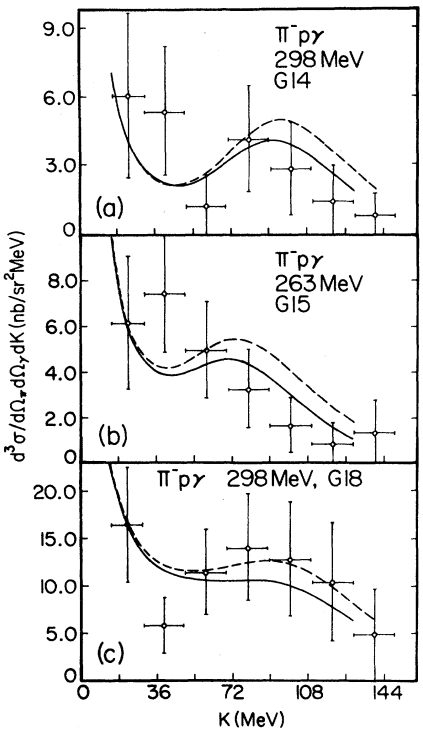

FIG. 14. The $\pi^- p\gamma$ cross section as a function of K (a) at 298 MeV for $G14$, (b) at 263 MeV for $G15$, and (c) at 298 MeV for $G18$. The solid curves and the dashed curves are explained in Fig. 13.

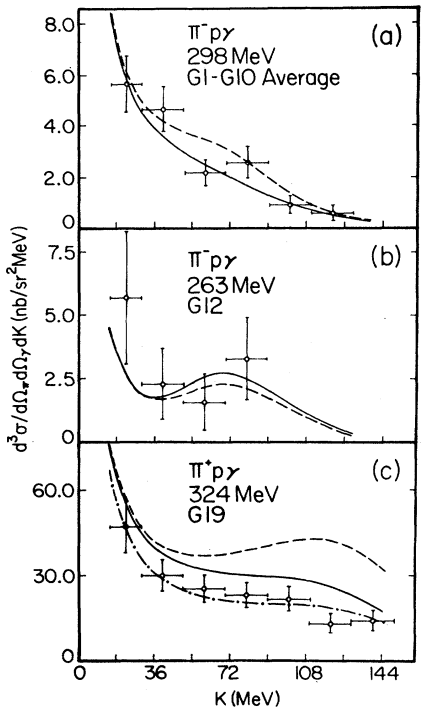

FIG. 13. (a) The average $\pi^- p\gamma$ cross section (over the ten photon counters $G1-G10$) as a function of K at 298 MeV. (b) The $\pi^- p\gamma$ cross section as a function of K at 263 MeV for $G12$. (c) Same as Fig. 9, but at 324 MeV for $G19$. The solid curves are calculated in the TETAS approximation using the amplitude M_μ(TETAS) and the dashed curves are calculated in the FYA approximation using the amplitude M_μ^{AB}(FYA) with the substitutions $p_{i\mu} \to p_{i\mu} - R_{i\mu}$ and $p_{f\mu} \to p_{f\mu} - R_{f\mu}$.

for many photon counters. But, again, the overall agreement between theory and experiment is better if the TETAS approximation is used. For the photon counter $G18$ at 298 MeV, the agreement between the TETAS calculation and the UCLA data is poor in the $\pi^+ p\gamma$ case [Fig. 12(c)] but the agreement is very good in the $\pi^- p\gamma$ case [Fig. 14(c)].

So far we have discussed only the soft-photon approximations. These approximations are model independent since the elastic T matrix, determined by the elastic scattering experiments, has been used as an input in the bremsstrahlung calculations. It should be pointed out that two model-dependent calculations, the Massachusetts Institute of Technology (MIT) model and the TRIUMF model, have been performed very recently by Heller *et al.*[14] and Wittman[15] in order to extract the magnetic moment of Δ^{++} from the $\pi^+ p\gamma$ data. Comparing with these model-dependent calculations, it is easy to find that the $\pi^+ p\gamma$ spectra calculated in the TETAS approximation are in better agreement with the experimental spectra obtained by the UCLA group than those calculated in either the MIT model or the TRIUMF model. A comparison between the calculation using the TETAS approximation and that using the MIT model is shown in Fig. 8.

The comparison between the predicted $p^{12}C\gamma$ cross sections and the experimental data is shown in Figs. 15 and 16 for the incident proton energies of 1.594, 1.81, 0.591, and 1.88 MeV. In the energy region far from any resonance, as shown in Fig. 15(a), all approximations give

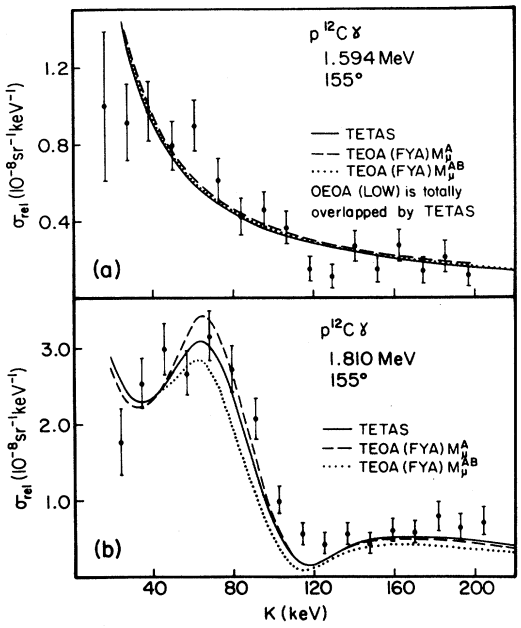

FIG. 15. The relative $p^{12}C\gamma$ cross section, σ_{rel}, as a function of photon energy K at the incident proton energies of (a) 1.594 MeV and (b) 1.81 MeV. The solid curves are the result of the calculation using the amplitude M_μ^{TETAS} given by Eq. (3) [or the amplitude M_μ(TETAS) given by Eq. (16)]. The dashed curves and the dotted curves are the result of the calculation using the amplitude M_μ^A(FYA) [Eq. (A1) in the Appendix] and the amplitude M_μ^{AB}(FYA) [Eq. (A2) in the Appendix], respectively. The experimental $p^{12}C\gamma$ data are from Ref. 3.

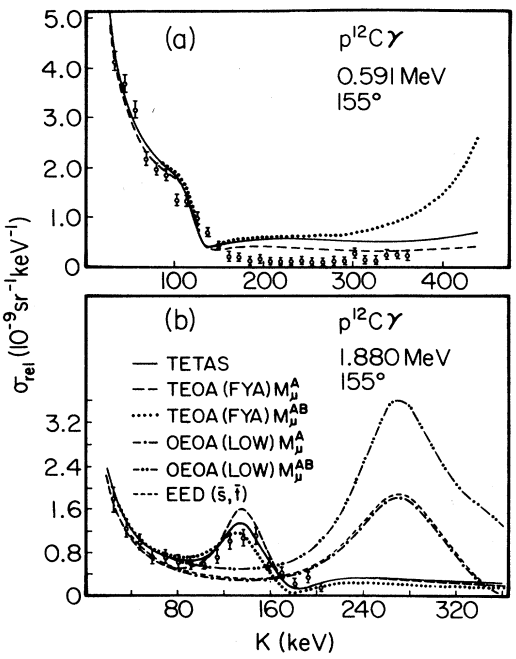

FIG. 16. Comparison of various theoretical predictions with the $p^{12}C\gamma$ data (the relative $p^{12}C\gamma$ cross section, σ_{rel}) at the incident proton energies of (a) 0.591 MeV and (b) 1.88 MeV. The solid curves are calculated in the TETAS approximation using either M_μ^{TETAS} or M_μ(TETAS). The long-dashed curves and the dotted curves are calculated in the FYA approximation using M_μ^A(FYA) and M_μ^{AB}(FYA), respectively. The dash-dotted curve and the dash-double-dotted curve are calculated in the Low approximation using M_μ^A(Low) (leading term only) and M_μ^{AB}(Low) (both leading term and the second term), respectively. The short-dashed curve is calculated in the EED approximation. The 0.591-MeV data are from Ref. 5 and the 1.88-MeV data are from Ref. 3.

about the same prediction and the result is in good agreement with the Brooklyn data.[3] In the vicinity of the 0.5-MeV and the 1.7-MeV resonances, both the TETAS approximation and the FYA approximation predict resonant structure which agrees very well with the observed one. This implies that the choice of the two energies, s_i and s_f (not any other linear combinations of s_i and s_f), used in both the TETAS amplitude and the FYA amplitude is correct. We refer to Ref. 20 for further discussion. Because of the finite size of the photon detector used in the experiment, the theoretical calculations should be averaged over the solid angle of the photon detector in order to compare with the experimental data. The result shown in Figs. 15 and 16 does not take into account the effects of the finite size of the photon detector. In general, the averaged cross sections are in much better agreement with the data than the unaveraged cross sections.

V. CONCLUSION

We have studied various bremsstrahlung amplitudes in the two-energy-two-angle approximation and have found two special two-energy-two-angle amplitudes, M_μ^{TETAS} and M_μ(TETAS), which depend only on the elastic T matrix evaluated at four sets of (s,t): (s_i,t_p), (s_f,t_p), (s_i,t_q), and (s_f,t_q). Here, M_μ^{TETAS} is the amplitude for the scattering of two spinless particles while M_μ(TETAS) is the amplitude for the scattering of a spin-0 particle and a spin-$\frac{1}{2}$ particle. The choice of these four sets of (s,t) is fixed by the requirement of making the amplitudes M_μ^{TETAS} and M_μ(TETAS) free of any term involving $\partial T/\partial s$ and/or $\partial T/\partial t$. Such choice is unique and can be done only in the TETA approximation. It turns out that these four sets of (s,t) are determined by the four external scattering diagrams. We have also discussed the reason (both the experimental evidence and the theoretical justification) for evaluating the elastic T matrix at either s_i or s_f but not at any other linear combination of s_i and s_f.

We have shown that the internal amplitude of M_μ^{TETAS} [viz., M_μ^I(TETAS)] represents the photon emission from the intermediate particle formed by two bombarding particles during the scattering and we have also proved that this internal amplitude is consistent with the soft-photon theorem, i.e., it is $0(K^0)$ and analytic at $K=0$.

The amplitude M_μ^{TETAS} and M_μ(TETAS) have been applied to calculate the $\pi^\pm p\gamma$ and the $p^{12}C\gamma$ cross sections. The result of this calculation has been compared with the experimental data and also with the result calculated in other soft-photon approximations (including Low, NLL,

EED, FYA, and FM approximations) and in MIT model of Heller *et al.* From this comparison, we have found that the amplitude M_μ(TETAS), which is better than any other amplitudes, can be used to describe almost all the available $\pi^\pm p\gamma$ and $p^{12}C\gamma$ data. Moreover, the amplitude $M_\mu^{\rm TETAS}$, which has a very simple expression, has also been found to be a very good approximation for bremsstrahlung processes with scattering resonances.

ACKNOWLEDGMENTS

We wish to thank Dr. B. F. Gibson for stimulating discussions. Sincere thanks are also due to Dr. L. C. Liu for providing the πp computer program. One of us (M.K.L.) is grateful for valuable discussions with Dr. L. Heller. This work was supported in part by the City University of New York Professional Staff Congress-Board of Higher Education Faculty Research Award Program.

APPENDIX: THE FESHBACH-YENNIE APPROXIMATION

The bremsstrahlung amplitude in the FYA has already been discussed in Ref. 23. The amplitude which involves only the principal (leading) term has the form

$$M_\mu^A(\mathrm{FYA})=\left[Z_A\frac{q_{f\mu}}{q_f\cdot K}+Z_B\frac{p_{f\mu}}{p_f\cdot K}-(Z_A+Z_B)\frac{(q_f+p_f)_\mu}{(q_f+p_f)\cdot K}\right]T(s_i,t)-T(s_f,t)\left[Z_A\frac{q_{i\mu}}{q_i\cdot K}+Z_B\frac{p_{i\mu}}{p_i\cdot K}-(Z_A+Z_B)\frac{(q_i+p_i)_\mu}{(q_i+p_i)\cdot K}\right], \tag{A1}$$

where

$$t=\lim_{k\to 0}t_p=\lim_{k\to 0}t_q\ .$$

The complete Feshbach-Yennie amplitude, which includes both the principal term and the correction (second) term, can be written as

$$M_\mu^{AB}(\mathrm{FYA})=M_\mu^A(\mathrm{FYA})+\left[Z_A\frac{q_{f\mu}}{q_f\cdot K}(X^p\cdot K)+Z_B\frac{p_{f\mu}}{p_f\cdot K}(X^q\cdot K)-Z_AX_\mu^p-Z_BX_\mu^q\right]\frac{\partial T}{\partial t}(s_i,t)-\frac{\partial T}{\partial t}(s_f,t)\left[Z_A\frac{q_{i\mu}}{q_i\cdot K}(X^p\cdot K)+Z_B\frac{p_{i\mu}}{p_i\cdot K}(X^q\cdot K)-Z_AX_\mu^p-Z_BX_\mu^q\right], \tag{A2}$$

where X_μ^p and X_μ^q are defined by the following equations:

$$(t_p-t)=X_\mu^pK^\mu+0(K^2)\ ,$$

$$(t_q-t)=X_\mu^qK^\mu+0(K^2)\ .$$

It is easy to show that the amplitude M_μ^{AB}(FYA) is exactly identical to Eq. (15) of Ref. 23.

The amplitudes M_μ^A(FYA) and M_μ^{AB}(FYA) have been used to calculate all $p^{12}C\gamma$ cross sections, shown in Figs. 15 and 16, since the contribution from the magnetic moment of proton is negligible. Some of the calculated $\pi^\pm p\gamma$ cross sections using these two amplitudes, compared with the TETAS calculations using the amplitude $M_\mu^{\rm TETAS}$ given by Eq. (3), are shown in Figs. 4–6. However, since the contribution from the magnetic moment of proton is not negligible for the $\pi^\pm p\gamma$ cases, we have used the modified M_μ^A(FYA) and M_μ^{AB}(FYA) in most of the $\pi^\pm p\gamma$ calculations (Figs. 7 and 9–14). The modified M_μ^A(FYA) and M_μ^{AB}(FYA) are obtained from Eqs. (A1) and (A2) by replacing every $p_{i\mu}$ and every $p_{f\mu}$ in the amplitude M_μ^A(FYA) [in both Eqs. (A1) and (A2)] by $p_{i\mu}-R_{i\mu}$ and $p_{f\mu}-R_{f\mu}$, respectively. Here, the expressions for $R_{i\mu}$ and $R_{f\mu}$ are defined by Eq. (14). In this work, the modified M_μ^A(FYA) and M_μ^{AB}(FYA) are always compared with the amplitude M_μ(TETAS) given by Eq. (16) while the original M_μ^A(FYA) and M_μ^{AB}(FYA) are compared with the amplitude $M_\mu^{\rm TETAS}$.

*Present address: Department of Physics, Central State University, Edmond, OK 73060.

[1]B. M. K. Nefkens *et al.*, Phys. Rev. D **18**, 3911 (1978), and references therein.

[2]C. Maroni *et al.*, Nucl. Phys. **A273**, 429 (1976).

[3]C. C. Trail, P. M. S. Lesser, A. H. Bond, Jr., M. K. Liou, and C. K. Liu, Phys. Rev. C **21**, 2131 (1980).

[4]H. Taketani, M. Adachi, N. Endo, and T. Suzuki, Phys. Lett. **113B**, 11 (1982).

[5]P. M. S. Lesser, C. C. Trail, C. C. Perng, and M. K. Liou, Phys. Rev. Lett. **48**, 308 (1982).

[6]C. C. Perng, D. Yan, P. M. S. Lesser, C. C. Trail, and M. K. Liou, Phys. Rev. C **38**, 514 (1988).

[7]M. I. Sobel and A. H. Cromer, Phys. Rev. **132**, 2698 (1963). An extensive list of references can be obtained from the following review articles: M. L. Halbert, in *Proceedings of Gull Lake Symposium on the Two-Body Force in Nuclei,* edited by S. M. Austin and G. M. Crawley (Plenum, New York, 1972); M. J. Moravcsik, Rep. Prog. Phys. **35**, 587 (1972); E. M. Nyman, Phys. Rep. **9**, 179 (1974); M. K. Liou, in *Proceedings of the International Conference on Few-Body Problems in Nuclear and Particle Physics, Quebec, Canada,* edited by R. J.

Slobodrian *et al.* (Les Presses de l'Universite Laval, Laval, Quebec, 1975); J. V. Jovanovich, *Nucleon-Nucleon Interactions—1977 (Vancouver),* Proceedings of the Second International Conference on Nucleon-Nucleon Interactions, AIP Conf. Proc. No. 41, edited by H. Fearing, D. Measday, and S. Strathdee (AIP, New York, 1977). For recent development in *pp,* see P. Kitching *et al.*, Phys. Rev. Lett. **57**, 2367 (1986); R. L. Workman and H. W. Fearing, Phys. Rev. C **34**, 780 (1986).

[8]R. M. Eisberg, D. R. Yennie, and D. H. Wilkinson, Nucl. Phys. **18**, 338 (1960).

[9]H. Feshbach and D. R. Yennie, Nucl. Phys. **37**, 150 (1962).

[10]F. Janouch and R. Mach, Nucl. Phys. **A158**, 193 (1970).

[11]A. M. Green, in *Proceedings of the International Conference on Few-Body Problems in Nuclear and Particle Physics, Quebec, Canada, 1974,* edited by R. J. Slobodrian *et al.* (Les Presses de l'Universite Laval, Laval, Quebec, 1975).

[12]N. M. Musakhanov, Yad. Fiz. **19**, 630 (1974) [Sov. J. Nucl. Phys. **19**, 319 (1974)].

[13]P. Pascual and R. Tarrach, Nucl. Phys. **B134**, 133 (1978).

[14]L. Heller, S. Kumans, J. C. Martinez, and E. J. Moniz, Phys. Rev. C **35**, 718 (1987).

[15]R. Wittman, Phys. Rev. C **37**, 2075 (1988).

[16]C. K. Liu, M. K. Liou, C. C. Trail, and P. M. S. Lesser, Phys. Rev. C **26**, 723 (1982).

[17]E. E. Low, Phys. Rev. **110**, 974 (1958).

[18]S. L. Adler and Y. Dothan, Phys. Rev. **151**, 1267 (1966).

[19]T. H. Burnett and N. M. Kroll, Phys. Rev. Lett. **20**, 86 (1968).

[20]M. K. Liou and Z. M. Ding, Phys. Rev. C **35**, 651 (1987).

[21]B. M. K. Nefkens and D. I. Sober, Phys. Rev. D **14**, 2434 (1976); B. M. K. Nefkens *et al.*, *ibid.* **18**, 3911 (1978).

[22]M. K. Liou and W. T. Nutt, Phys. Rev. D **16**, 2176 (1977); Nuovo Cimento **46A**, 365 (1978); M. K. Liou and C. K. Liu, Phys. Rev. D **26**, 1635 (1982).

[23]M. K. Liou, C. K. Liu, P. M. S. Lesser, and C. C. Trail, Phys. Rev. C **21**, 518 (1980); H. Feshbach and D. R. Yennie, Nucl. Phys. **37**, 150 (1962).

[24]W. E. Fischer and P. Minkowski, Nucl. Phys. **B36**, 519 (1972).

[25]L. Heller, in *Few Body Systems and Nuclear Forces II,* Vol. 87 of *Lecture Notes in Physics,* edited by H. Zingl, M. Haftel, and H. Zankel (Springer-Verlag, Berlin, 1978), p. 68.

[26]Z. M. Ding and M. K. Liou, Mod. Phys. Lett. **A3**, 1065 (1988).

[27]S. J. Brodsky and R. W. Brown, Phys. Rev. Lett. **49**, 966 (1982); R. W. Brown, K. L. Kowalski, and S. J. Brodsky, Phys. Rev. D **28**, 624 (1983).

[28]Our proof given in last paragraph can also be applied to show that the internal amplitude (the sum of the gauge terms) used by Liou and Cho [Nucl. Phys. **A124**, 85 (1969)] has the right analytic structure and hence is consistent with the soft-photon theorem. The comment made by Workman and Fearing [Phys. Rev. C **34**, 782 (1986)] is incorrect.